Propofol reduces lipopolysaccharide-induced cardiomyocyte injury in sepsis by activating SIRT1-mediated autophagy

JUNWANG DU[1] and YAN ZHOU[2]

[1]Department of Anesthesiology, Tianshui First People's Hospital, Tianshui, Gansu 741000;
[2]Department of Critical Care Medicine, The Third Affiliated Hospital of Guangzhou Medical University, Guangzhou, Guangdong 510150, P.R. China

Received June 20, 2022; Accepted September 14, 2022

DOI: 10.3892/etm.2023.11886

Abstract. Myocardial injury is an indicator of poor prognosis in sepsis, whereas propofol has been reported to protect the myocardium. Therefore, the present study investigated the effect of propofol on myocardial injury in sepsis and its mechanism. An *in vitro* model of myocardial cell injury was established in myocardial H9C2 cells using lipopolysaccharide (LPS). The Cell Counting Kit 8 (CCK8) assay was used to investigate the effect of propofol pretreatment on the viability of normal and LPS-challenged H9C2 cells, whereas the lactate dehydrogenase (LDH) detection kit was used to measure the levels of LDH. The expression levels of LC3 were analyzed using an immunofluorescence assay. Western blotting was performed to analyze the expression levels of autophagy-related proteins. Following treatment with the autophagy inhibitor 3-methyladenine, CCK8 assay, TUNEL assay, western blotting, 2,7-dichlorohydrofluorescein diacetate assay and ELISA were performed to investigate whether propofol exerted its effects on cell viability, apoptosis, oxidative stress and inflammation via autophagy. Moreover, to further explore the regulatory mechanism of propofol in myocardial injury, sirtuin 1 (SIRT1) was knocked down via transfection with small interfering RNA, and SIRT1 protein was inhibited via the addition of the SIRT1 inhibitor EX527. The present study demonstrated that propofol activated autophagy in LPS-induced cardiomyocytes, and reversed the effects of LPS on viability, apoptosis, oxidative stress and the inflammatory response. Moreover, SIRT1 knockdown and inhibition decreased the activation of autophagy and the protective effect of propofol on LPS-induced cardiomyocytes. In conclusion, propofol reduced LPS-induced cardiomyocyte injury by activating SIRT1-mediated autophagy.

Correspondence to: Dr Yan Zhou, Department of Critical Care Medicine, The Third Affiliated Hospital of Guangzhou Medical University, 63 Duobao Road, Guangzhou, Guangdong 510150, P.R. China
E-mail: zhouyanzy8@126.com

Key words: cardiomyocyte injury, sepsis, propofol, autophagy, sirtuin 1

Introduction

Multiple organ dysfunction caused by sepsis and septic shock is an important issue in acute and critical care. Sepsis-induced myocardial injury is the most common complication of organ dysfunction (1). Among adult patients with sepsis, 25-50% of them present with myocardial injury, which is an indicator of poor prognosis of sepsis and can increase the mortality rate to 70% (2). Therefore, active treatment of sepsis-induced myocardial injury is necessary to improve the survival rate and prognosis of patients.

Propofol is the most commonly used intravenous anesthetic in clinical practice (3). Previous studies have reported that propofol has a protective effect on the myocardium (4-6). Propofol mediates cardioprotective effects against myocardial ischemia/reperfusion injury in a microRNA-451/high mobility group box 1 (HMGB1)-dependent manner (4), alleviates doxorubicin-induced toxic injury through activation of Nrf2/GPx4 signaling (5), and protects the myocardium from ischemia-reperfusion injury by inhibiting ferroptosis through the AKT/p53 signaling pathway (6). These results suggested that propofol may have important protective effects on cardiac function. In addition, a previous study revealed that propofol significantly improves the survival rate of rats with sepsis, and has protective effects on the liver, kidneys and heart (7). Moreover, a recent study demonstrated that propofol inhibits inflammation and apoptosis through the PPARγ/HMGB1/NLRP3 axis to improve endotoxin-induced cardiomyocyte injury (8). These results indicated that propofol may participate in the protective effects against septic injury through multiple pathways.

It has been shown that propofol effectively activates sirtuin 1 (SIRT1), and reduces lung injury, liver injury and human umbilical vein endothelial cell injury induced by high glucose (9-11). SIRT1 is a key regulator of autophagy, which has recently been recognized as a new selective substrate for nuclear autophagy in senescence and aging (12). SIRT1 promotes autophagy through AMPK activation, thereby protecting cardiomyocytes from hypoxia (13). Melatonin regulates apoptosis and autophagy by activating SIRT1 in mice to prevent heart dysfunction induced by sepsis (14). In addition, it has been shown that propofol has an important regulatory effect on autophagy, thus affecting cellular homeostasis (15).

The present study hypothesized that propofol may activate SIRT1-mediated autophagy in lipopolysaccharide (LPS)-induced myocardial injury and aimed to investigate this hypothesis *in vitro*.

Materials and methods

Cell culture. The rat cardiomyocyte H9C2 cells (MilliporeSigma) were cultured in DMEM supplemented with 10% FBS (both from Gibco; Thermo Fisher Scientific, Inc.) at 37˚C in an atmosphere containing 5% CO_2. Cells were sub-cultured when they reached 90% confluence. For the *in vitro* sepsis-induced myocardial injury model, H9C2 cells were sub-cultured for 12 h and then induced with LPS (1 μg/ml; cat. no. HY-D1056; MedChemExpress) for 24 h at 37˚C (16). Concentrations of 12.5, 25 and 50 μM propofol (cat. no. HY-B0649; MedChemExpress) were selected to pretreat H9C2 cells at 37˚C for 24 h prior to LPS treatment (8,17). In the inhibition experiments, cell were pre-treated for 30 min with the autophagy inhibitor 3-methyladenine (3-MA; 10 μM; cat. no. HY-19312; MedChemExpress) and the SIRT1 inhibitor EX527 (100 nM; cat. no. HY-15452; MedChemExpress) at 37˚C, followed by LPS induction and propofol treatment (18,19). Untreated H9C2 cells were regarded as the control group.

Cell Counting Kit 8 (CCK8) assay. The viability of H9C2 cells was measured using the CCK8 assay (Nanjing Jiancheng Bioengineering Institute), according to the manufacturer's instructions. The absorbance was measured at a wavelength of 450 nm using a microplate reader (Thermo Fisher Scientific, Inc.).

Immunofluorescence (IF) analysis. After treatment, H9C2 cells were fixed with 4% paraformaldehyde in PBS for 30 min at room temperature. Subsequently, cells were washed and incubated with 0.2% Triton X-100 (MilliporeSigma) for 10 min at room temperature. The cells were then incubated with 5% goat serum (MilliporeSigma) for 30 min at room temperature and with a primary antibody against LC3 (cat. no. ab192890; 1:2,000; Abcam) overnight at 4˚C. Following primary antibody incubation, cells were incubated with goat anti-rabbit IgG H&L (Alexa Fluor® 488; cat. no. ab150077; 1:200; Abcam) at room temperature for 1 h. DAPI was used to stain the cell nuclei for 5 min at room temperature and images were captured using a confocal laser scanning microscopy (Zeiss AG).

Western blotting. Proteins were extracted from cells on ice with RIPA buffer (Beyotime Institute of Biotechnology) and protein concentrations were determined using a BCA kit (MilliporeSigma). Total proteins (~30 μg/lane) were separated by SDS-PAGE on a 10% gel and were transferred onto a PVDF membrane (Bio-Rad Laboratories, Inc.). After blocking for 1 h in 5% skim milk, the membranes were incubated with the primary antibodies against SIRT1 (cat. no. ab189494; 1:1,000; Abcam), LC3 (cat. no. ab192890; 1:2,000; Abcam), Beclin-1 (cat. no. ab207612; 1:2,000; Abcam), p62 (cat. no. ab109012; 1:10,000; Abcam), Bcl-2 (cat. no. ab196495; 1:1,000; Abcam), Bax (cat. no. ab32503; 1:1,000; Abcam), cleaved caspase-3 (cat. no. #9661; 1:1,000; Cell Signaling Technology, Inc.), caspase-3 (cat. no. ab184787; 1:2,000; Abcam), phosphorylated (p)-p65 (cat. no. ab76302; 1:1,000; Abcam), p65 (cat. no. #8242; 1:1,000; Cell Signaling Technology, Inc.), iNOS (cat. no. ab178945; 1:1,000; Abcam), COX-2 (cat. no. ab179800; 1:1,000; Abcam) and GAPDH (cat. no. ab181602 1:10,000; Abcam) overnight at 4˚C. Following primary antibody incubation, the membranes were incubated with the appropriate horseradish peroxidase-conjugated secondary antibody (cat. no. ab6721; 1:2,000; Abcam) at room temperature for 2 h and visualized using the Pierce™ ECL Western Blotting Substrate (Thermo Fisher Scientific, Inc.). Protein bands were analyzed with Quantity One® software version 4.5 (Bio-Rad Laboratories, Inc.).

Reverse transcription-quantitative PCR (RT-qPCR). Total RNA was isolated from cells using TRIzol® reagent (Invitrogen; Thermo Fisher Scientific, Inc.), according to the manufacturer's instructions. RNA was reverse-transcribed into cDNA using a Primescript™ RT reagent kit (Invitrogen; Thermo Fisher Scientific, Inc.) according to the manufacturer's instructions. The synthesized cDNA was amplified and quantified using the Real-time PCR Master Mix (SYBR Green) kit (cat.no. KGA1339-1; Nanjing KeyGen Biotech Co., Ltd.). GAPDH was used as an internal reference for evaluating the relative expression of SIRT1. The thermocycling conditions were as follows: Denaturation at 94˚C for 2 min; followed by 30 cycles at 94˚C for 30 sec, 56˚C for 30 sec and 72˚C for 30 sec; and a final elongation step at 72˚C for 5 min. Relative expression levels were calculated using the $2^{-\Delta\Delta Cq}$ method (20). The following primer pairs were used for qPCR: SIRT1 forward, 5'-ATCTCCCAGATCCTCAAGCCA-3' and reverse, 5'-CTTCCACTGCACAGGCACAT-3'; and GAPDH forward, 5'-GCATCTTCTTGTGCAGTGCC-3' and reverse, 5'-GAT GGTGATGGGTTTCCCGT-3'.

TUNEL assay. H9C2 cells ($2x10^6$/ml) were fixed in 4% paraformaldehyde for 15 min at room temperature, and were then washed and incubated with 0.2% Triton X-100 (Sigma-Aldrich; Merck KGaA) for 20 min at room temperature. Cells were incubated with 50 μl TUNEL reaction mixture (cat. no. 11684817910; MilliporeSigma) at 37˚C for 60 min in the dark. The cells were then incubated with DAPI at room temperature for 10 min, washed with PBS, mounted in glycerol and visualized with a fluorescence microscope (five fields).

2,7-dichlorohydrofluorescein diacetate (DCFH-DA) assay. Reactive oxygen species (ROS) levels were measured by staining with the fluorescent probe DCFH-DA (Beyotime Institute of Biotechnology), according to the manufacturer's instructions. Following drug treatments, cells were stained in the dark with DCFH-DA (10 μM) in DMEM at 37˚C for 30 min. Images of the stained cells were captured under a fluorescence microscope (Olympus Corporation) using excitation and emission wavelengths of 488 and 525 nm, respectively.

Glutathione peroxidase (GSH-Px) activity, malondialdehyde (MDA) content and superoxide dismutase (SOD) activity detection. H9C2 cells maintained in PBS were centrifuged at 1,500 x g for 10 min at 4˚C and the cell supernatants were then collected. The GSH-Px activity, MDA contents and SOD activity in the cell supernatants were measured using the GSH-Px assay kit (cat. no. A005-1-2), MDA assay kit (cat. no. A003-1-2) and SOD assay kit (cat. no. A001-3-2),

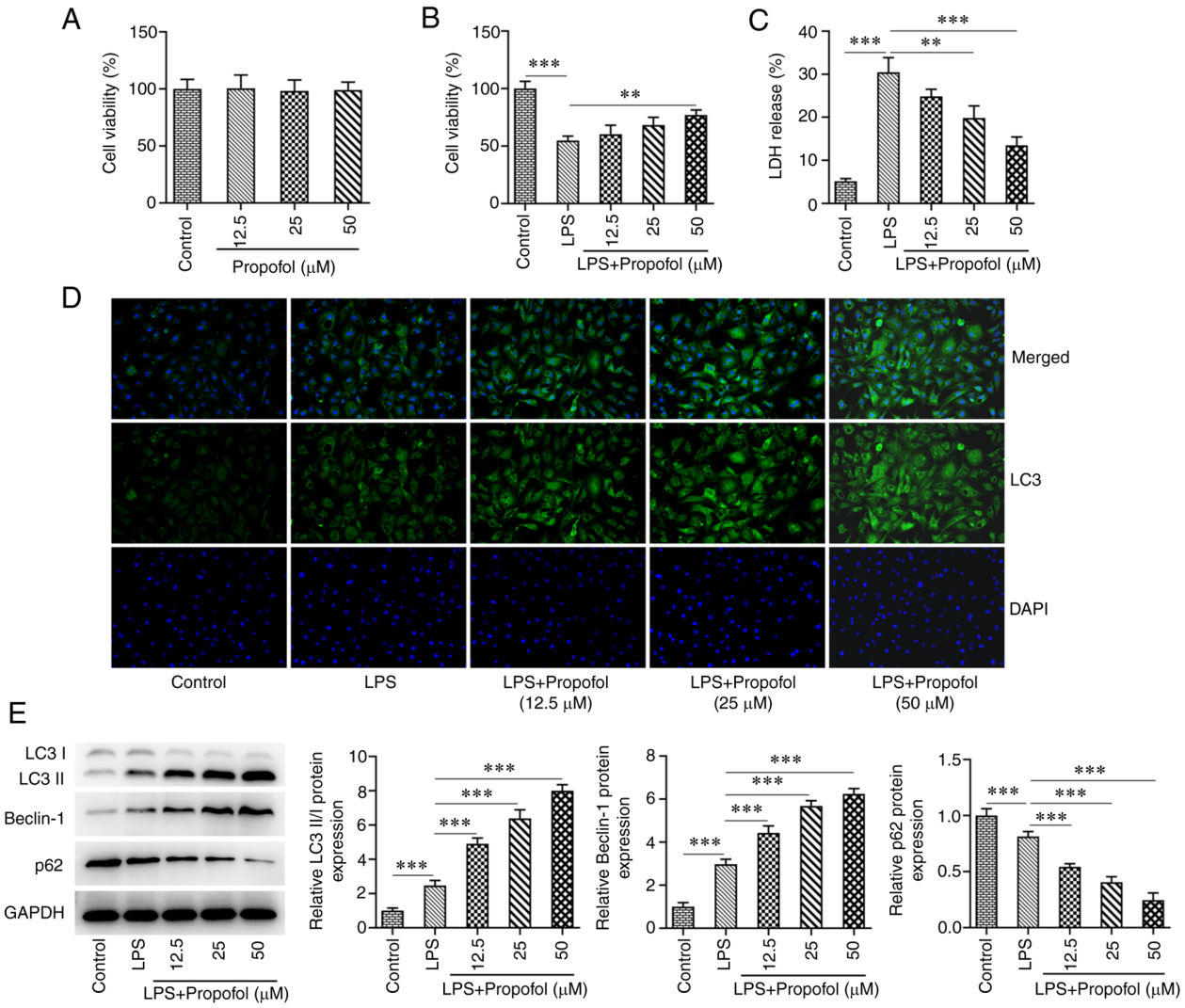

Figure 1. Propofol activates autophagy in LPS-induced cardiomyocytes. (A and B) Cell viability was measured using the Cell Counting Kit 8 assay. (C) Levels of LDH were detected using the LDH kit. (D) Immunofluorescence analysis of the expression of LC3. Magnification, x200. (E) Western blot analysis of the expression levels of LC3II/1, Beclin1 and p62. **P<0.01, ***P<0.001. LPS, lipopolysaccharide; LDH, lactate dehydrogenase.

respectively, according to the manufacturer's instructions (Nanjing Jiancheng Bioengineering Institute).

ELISA. H9C2 cells maintained in PBS were centrifuged at 1,500 x g for 10 min at 4°C and the cell supernatants were then collected. The levels of TNF-α, IL-6, IL-1β and lactate dehydrogenase (LDH) in the supernatants of H9C2 cells after different treatments were measured using the TNF-α assay kit (cat. no. H052-1-2), IL-6 assay kit (cat. no. H007-1-1), IL-1β assay kit (cat. no. H002-1-2) and LDH assay kit (cat. no. A020-2-2), respectively, according to the manufacturer's protocols (Nanjing Jiancheng Bioengineering Institute).

Cell transfection. H9C2 cells seeded into 6-well plates at a density of $1x10^6$ cells/well were transfected with 100 nM non-targeting small interfering RNA (siRNA)-negative control (si-NC), si-SIRT1-1 or si-SIRT2-2 (all purchased from Shanghai GenePharma Co., Ltd.) for 48 h at 37°C with Lipofectamine® RNAiMAX (Invitrogen; Thermo Fisher Scientific, Inc.), according to the manufacturer's protocol. Post-transfection, cells were used for subsequent functional experiments 48 h post-transfection. The siRNA sequences were as follows: si-SIRT1-1 sense, 5'-AAAACUUAACUCUAACGACAA-3' and antisense, 5'-GUCGUUAGAGUUAAGUUUUUC-3'; si-SIRT1-2 sense, 5'-UUUAGGAAUAGCUCUUUCCUU-3' and antisense, 5'-GGAAAGAGCUAUUCCUAAAAC-3'; and si-NC sense, 5'-UUCUCCGAACGUGUCACGUTT-3' and antisense, 5'-ACGUGACACGUUCGGAGAATT-3'.

Statistical analysis. Data are presented as the mean ± standard derivation. Statistical analyses were performed using one-way ANOVA followed by Tukey's post hoc test in GraphPad Prism 8 (GraphPad Software, Inc.). P<0.05 was considered to indicate a statistically significant difference.

Results

Propofol activates autophagy in LPS-induced cardiomyocyte injury. H9C2 cells were treated with 12.5, 25 and 50 μM propofol, and the CCK8 assay showed no significant difference in the viability of H9C2 cells at this concentration range compared with in the control group (Fig. 1A). By contrast, cell

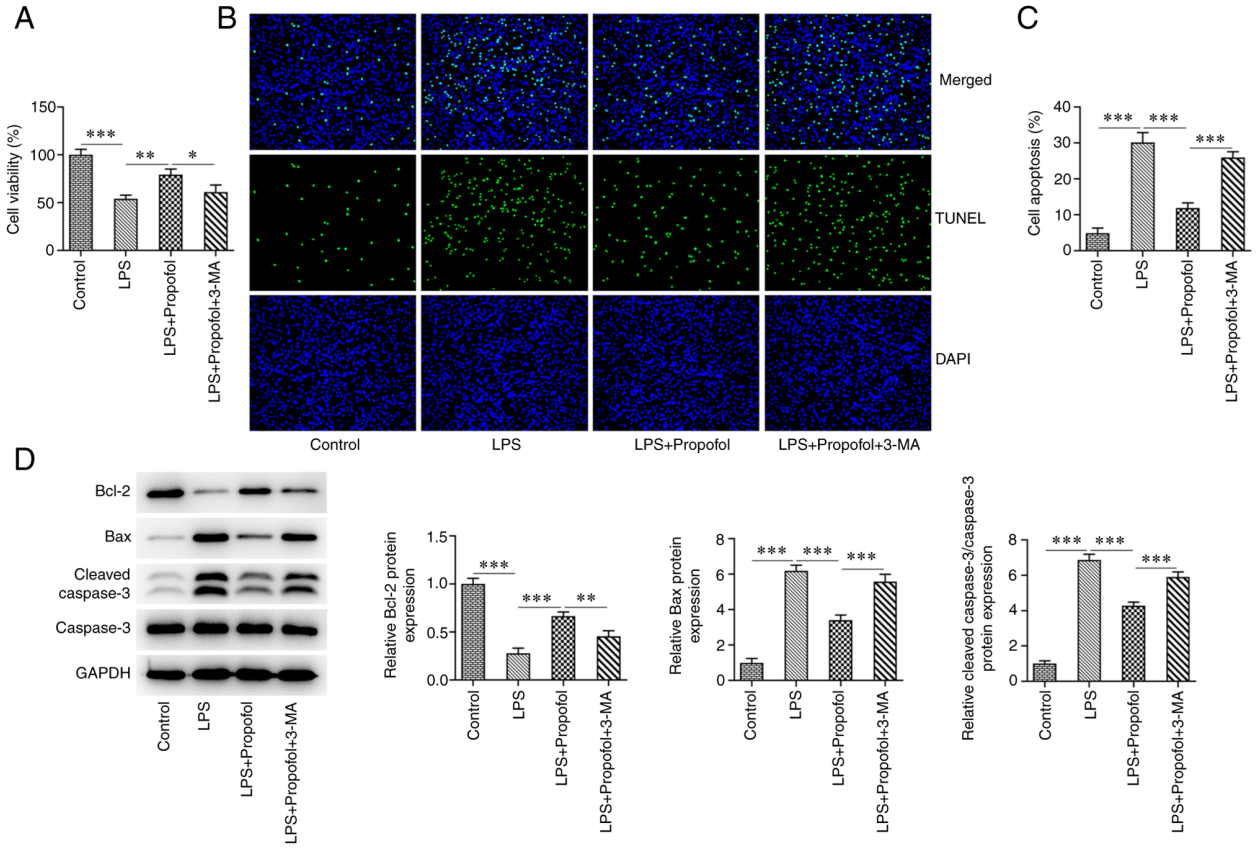

Figure 2. Propofol reduces LPS-induced decreases in cardiomyocyte viability and apoptosis by activating autophagy. (A) Cell viability was measured using the Cell Counting Kit 8 assay. (B) Cell apoptosis was measured using the TUNEL assay. Magnification, x200. (C) Percentage of apoptotic cells. (D) Western blot analysis of the expression levels of Bcl-2, Bax, cleaved caspase-3 and caspase-3. *P<0.05, **P<0.01, ***P<0.001. LPS, lipopolysaccharide; 3-MA, 3-methyladenine.

viability was significantly decreased following LPS induction compared with in the control group. Compared with in the LPS group, cell viability in the LPS + propofol groups was increased, with a significant increase detected in response to 50 μM propofol (Fig. 1B). The levels of LDH in the cell supernatants were significantly increased in the LPS group compared with those in the control group, whereas LDH levels were significantly decreased in the LPS + 25 μM propofol and LPS + 50 μM propofol groups compared with those in the LPS group (Fig. 1C). IF assay revealed that LC3 expression was markedly increased following LPS induction. Compared with in the LPS group, LC3 expression was further increased in all of the LPS + propofol groups in a concentration-dependent manner (Fig. 1D). Western blot analysis demonstrated that the expression levels of LC3II/I and Beclin-1 were increased in the LPS group, whereas the expression of p62 was decreased compared with that in the control group. Compared with in the LPS group, LC3II/I and Beclin-1 expression levels were further increased and p62 expression was further decreased in all of the LPS + propofol groups (Fig. 1E). Propofol (50 μM) was selected for subsequent experiments since it exhibited a greater effect on the expression of autophagy-related markers.

Propofol reduces LPS-induced apoptosis and decreases in cardiomyocyte viability by activating autophagy. To further investigate whether 50 μM propofol regulated myocardial cell injury by activating autophagy, cells were pre-treated with the autophagy inhibitor 3-MA. Cell viability was significantly decreased in the LPS + propofol + 3-MA group compared with that in the LPS + 50 μM propofol group (Fig. 2A). The TUNEL assay indicated that LPS exposure significantly potentiated H9C2 cell apoptosis, whereas the apoptosis in the LPS + 50 μM propofol + 3-MA group was significantly increased compared with that in the LPS + 50 μM propofol group (Fig. 2B and C). Furthermore, western blotting revealed that LPS treatment significantly reduced Bcl-2 expression, and elevated Bax and cleaved caspase-3 expression. Also, the expression levels of Bax and cleaved caspase-3 were increased, whereas the expression levels of Bcl-2 were decreased in the LPS + 50 μM propofol + 3-MA group compared with those in the LPS + 50 μM propofol group (Fig. 2D).

Propofol reduces LPS-induced oxidative stress and inflammatory damage in cardiomyocytes by activating autophagy. ROS levels were detected by DCFH-DA staining. Notably, DCFH-DA staining, and thus ROS generation, was markedly increased in the LPS group compared with that in the control group, whereas it was decreased in the LPS + 50 μM propofol group. By contrast, ROS generation was higher in the LPS + 50 μM propofol + 3-MA group than that in the LPS + 50 μM propofol group (Fig. 3A). Subsequently, the levels of oxidative stress markers, MDA, SOD and GSH-Px, were assessed. The MDA levels were significantly increased in the LPS group compared with those in the control group, whereas SOD and

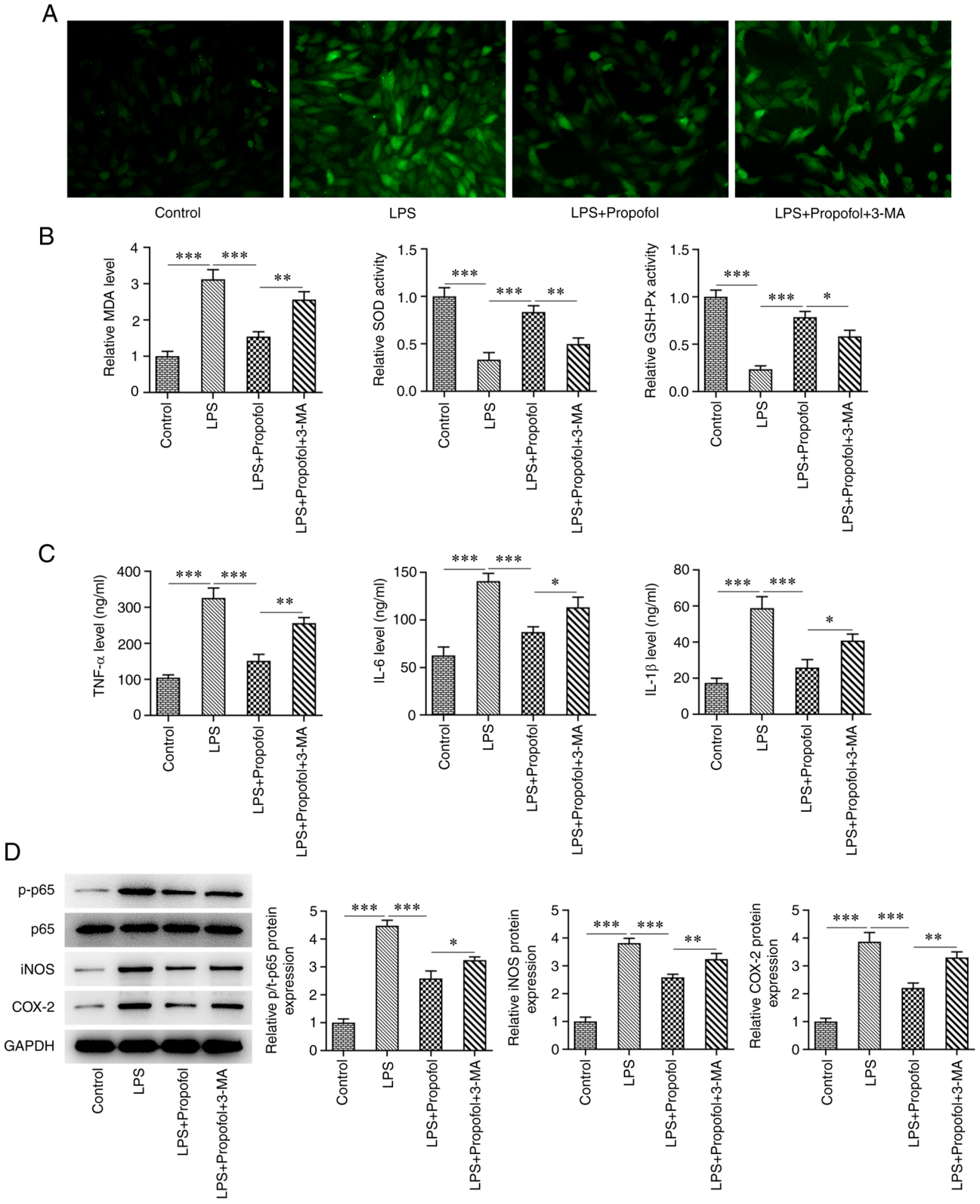

Figure 3. Propofol reduces LPS-induced oxidative stress and inflammatory damage in cardiomyocytes by activating autophagy. (A) 2,7-dichlorohydrofluorescein diacetate staining assay for the detection of reactive oxygen species generation. Magnification, x200. (B) Levels of MDA content, SOD and GSH-Px activities. (C) ELISA of the levels of TNF-α, IL-6 and IL-1β. (D) Western blot analysis of the expression levels of p65, p-p65, iNOS and COX-2. *P<0.05, **P<0.01, ***P<0.001. LPS, lipopolysaccharide; GSH-Px, glutathione peroxidase; MDA, malondialdehyde; SOD superoxide dismutase; p-, phosphorylated; 3-MA, 3-methyladenine.

GSH-Px activities were significantly decreased. Compared with in the LPS group, the levels of MDA were significantly decreased in the LPS + 50 μM propofol group, whereas the activities of SOD and GSH-Px were significantly increased. Compared with in the LPS + 50 μM propofol group, the MDA levels were significantly increased in the LPS + 50 μM

propofol + 3-MA group, whereas the SOD and GSH-Px activities were significantly decreased (Fig. 3B). The levels of TNF-α, IL-6 and IL-1β, which were measured via ELISA, were significantly increased following LPS induction compared with those in the control group. Compared with in the LPS group, TNF-α, IL-6 and IL-1β levels were significantly decreased in the LPS + 50 μM propofol group. By contrast, a significant increase in TNF-α, IL-6 and IL-1β levels was observed in the LPS + 50 μM propofol + 3-MA group compared with in the LPS + 50 μM propofol group (Fig. 3C). Western blot analysis showed a significant increase in the expression levels of inflammatory enzymes, including iNOS, p-p65 and COX-2, in the LPS group compared with those in the control group, whereas the expression levels of these proteins were decreased in the LPS + 50 μM propofol group. Conversely, a significant increase in the expression levels of iNOS, p-p65 and COX-2 was observed in the LPS + 50 μM propofol + 3-MA group compared with in the LPS + 50 μM propofol group (Fig. 3D).

Inhibition of SIRT1 reduces propofol-activated autophagy in LPS-induced cardiomyocytes. Cells were transfected with either si-SIRT1-1 or si-SIRT1-2, and exhibited a significant decrease in the mRNA and protein expression levels of SIRT1 (Fig. 4A and B). Notably, si-SIRT1-2 exerted the greatest effect on SIRT1 expression and was thus chosen for subsequent experiments. In addition, the SIRT1 inhibitor EX527 was also used to inhibit SIRT1. The IF assay revealed that the expression levels of LC3 in the LPS + 50 μM propofol + si-SIRT1 group were markedly decreased compared with those in the LPS + 50 μM propofol + si-NC group. Compared with in the LPS + 50 μM propofol group, the expression levels of LC3 were also markedly decreased in the LPS + 50 μM propofol + EX527 group (Fig. 4C). Western blot analysis revealed a significant decrease in the expression levels of LC3II/I and Beclin-1 in the LPS + 50 μM propofol + si-SIRT1 group compared with those in the LPS + 50 μM propofol + si-NC group, whereas the expression of p62 was significantly increased. In addition, compared with in the LPS + 50 μM propofol group, the expression levels of LC3II/I and Beclin-1 were significantly decreased, whereas the expression of p62 was significantly increased in the LPS + 50 μM Propofol + EX527 group (Fig. 4D).

Inhibition of SIRT1 reduces the protective effect of propofol on LPS-induced cardiomyocytes. The CCK8 assay showed that cell viability in the LPS + 50 μM propofol + si-SIRT1 group was significantly decreased compared with that in the LPS + 50 μM propofol + si-NC group. Compared with in the LPS + 50 μM propofol group, cell viability in the LPS + 50 μM propofol + EX527 group was also significantly decreased (Fig. 5A). The TUNEL assay revealed that apoptosis was significantly increased in the LPS + 50 μM propofol + si-SIRT1 group compared with that in the LPS + 50 μM propofol + si-NC group. Compared with in the LPS + 50 μM propofol group, apoptosis was also significantly increased in the LPS + 50 μM propofol + EX527 group (Fig. 5C). The results of western blotting showed that the expression levels of Bax and cleaved caspase-3 were significantly increased in the LPS + 50 μM propofol + si-SIRT1 group compared with in the LPS + 50 μM propofol + si-NC group, whereas Bcl-2 expression was significantly decreased. Similar results were obtained in the LPS + 50 μM propofol + EX257 group compared with in the LPS + 50 μM propofol group (Fig. 5D). ROS generation in the LPS + 50 μM propofol + si-SIRT1 group was markedly higher than that in the LPS + 50 μM propofol + si-NC group (Fig. 5E). Compared with in the LPS + 50 μM propofol + si-NC group, the MDA levels in the LPS + 50 μM propofol + si-SIRT1 group were significantly increased, whereas a significant decrease in the SOD and GSH-Px activities was observed (Fig. 5F). The trend of oxidative stress factors in the LPS + 50 μM propofol + EX527 group was consistent with that in the LPS + 50 μM propofol + si-SIRT1 group (Fig. 5E and F). ELISA showed that, compared with those in the LPS + 50 μM propofol + si-NC groups, the levels of TNF-α, IL-6 and IL-1β were significantly increased in the LPS + 50 μM propofol + si-SIRT1 group. Similarly, TNF-α, IL-6 and IL-1β levels were significantly increased in the LPS + 50 μM propofol + EX527 group compared with those in the LPS + 50 μM propofol group (Fig. 5G). Furthermore, western blot analysis indicated that, compared with those in the LPS + 50 μM propofol + si-NC group, the expression levels of iNOS, p-p65 and COX-2 were significantly increased in the LPS + 50 μM propofol + si-SIRT1 group. Similarly, iNOS, p-p65 and COX-2 expression levels were significantly increased in the LPS + 50 μM propofol + EX527 group compared with those in the LPS + 50 μM propofol group (Fig. 5E).

Discussion

Severe sepsis can lead to organ dysfunction, with heart dysfunction being the most common type (21). Therefore, ameliorating cardiac dysfunction and myocardial injury after sepsis can improve the prognosis of patients. Endotoxin is a toxic component of LPS, which can significantly promote inflammation and the immune response (22). Previous studies have shown that when LPS enters the body, free LPS can interact with immune cells and induce the release of inflammatory mediators, pro-apoptotic factors and pro-fibrotic factors, thus leading to abnormalities in coronary arteries, directly damaging myocardial cells, affecting cardiac function (23), and eventually resulting in myocardial fibrosis and cardiac disease, such as myocardial infarction (24,25). In the present study, H9C2 cells were induced by LPS treatment to create a model of myocardial cell injury *in vitro*. The present results showed that H9C2 cells underwent oxidative stress and inflammatory injury following LPS induction, with decreased cell viability and increased apoptosis.

The Increased generation of ROS activates the antioxidant system (26). MDA is a lipid peroxidation product that is widely detected as an oxidative stress marker (27). The antioxidant GSH can prevent ROS-induced cell damage; notably, all cells in the human body are able to synthesize GSH, which is essential for protection against oxidative stress (28). A decrease in SOD activity can result in the accumulation of peroxides, which can also lead to oxidative stress (29,30). Therefore, the present study investigated the levels of oxidative stress markers, ROS, MDA, SOD and GSH-Px, in H9C2 cells and revealed that, following LPS induction, the levels of ROS and MDA were increased, whereas the activities of SOD and GSH-Px were decreased, indicating that the level of oxidative stress was increased after LPS induction. TNF-α is considered a key regulator of the inflammatory

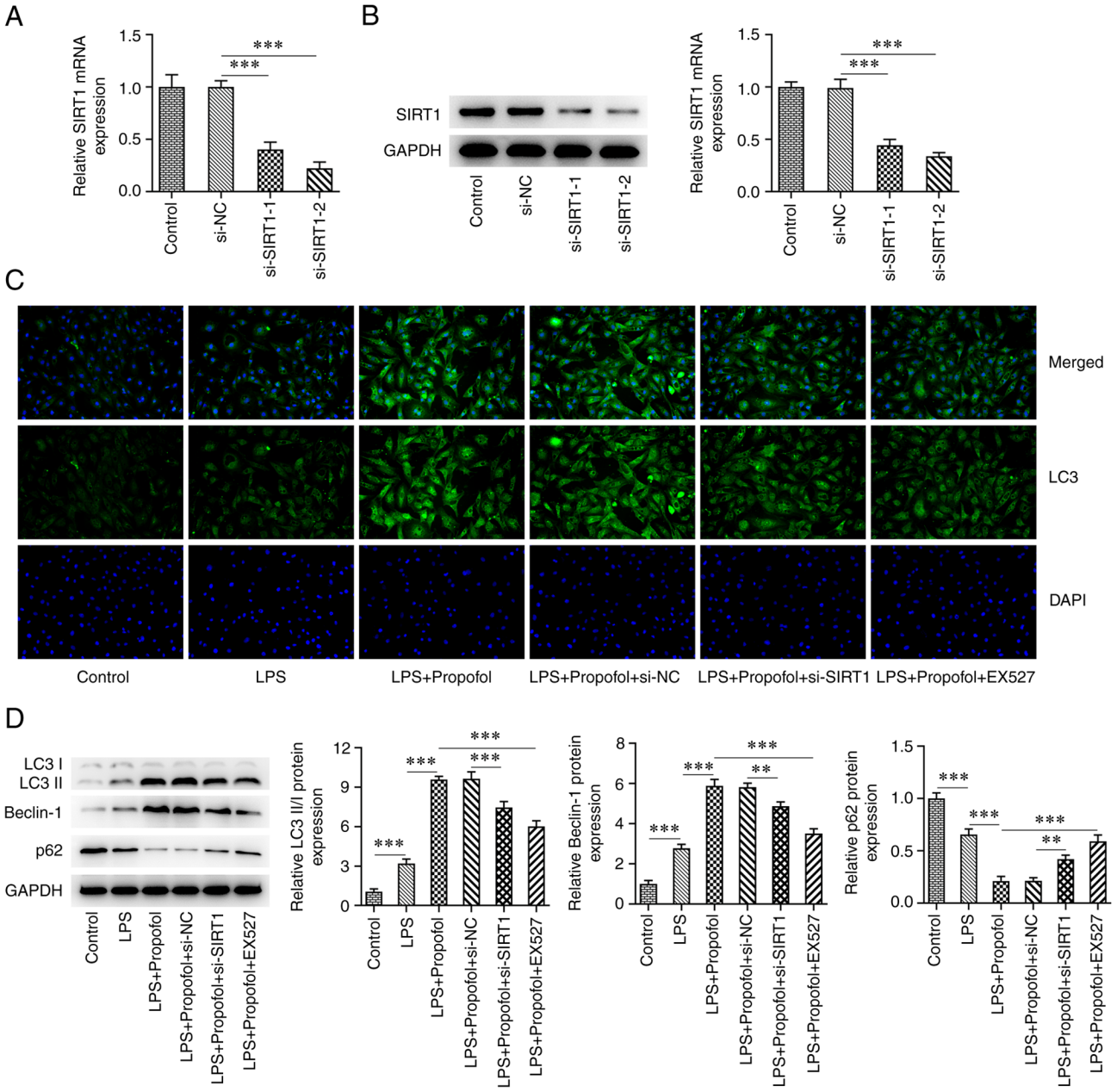

Figure 4. Inhibition of SIRT1 reduces propofol-activated autophagy in LPS-induced cardiomyocytes. (A) Reverse transcription-quantitative PCR and (B) western blot analysis of the expression levels of SIRT1. (C) Immunofluorescence analysis of the expression of LC3. Magnification, x200. (D) Western blot analysis of the expression levels of LC3II/I, Beclin1 and p62. **P<0.01, ***P<0.001. LPS, lipopolysaccharide; SIRT1, sirtuin 1; NC, negative control; si, small interfering.

response that is released when the body is injured (31). Moreover, IL-1β and IL-6 are important pro-inflammatory cytokines that are related to several autoimmune diseases and have a key role following infection (32). In the present study, following LPS induction, the levels of TNF-α, IL-6 and IL-1β were increased, indicating the activation of an inflammatory response. Autophagy is an important self-protection mechanism of cells, which aims to decompose intracellular protein macromolecules and organelles into small molecules for recycling, in order to maintain the metabolic process of cells upon exposure to various stimulating factors, including oxidative stress and toxin stimulation, and improve cell survival (33). The level of autophagy is low under normal physiological conditions and autophagy can be activated by several factors, such as nutrient deficiency, hypoxia, infection, tumorigenesis, tissue damage, protein misfolding, DNA damage, radiotherapy and chemotherapy (34). Autophagy can be observed in the early stage of sepsis via detection of the aggregation of autophagy-related proteins (LC3II/I, Beclin1 and p62) and the formation of autophagosomes (35). MicroRNA-155 has been reported to alleviate septic lung injury by inhibiting transforming growth factor-β-activated binding protein 2 and thus inducing autophagy (36). The present study indicated that autophagy may be activated to protect cells from damage following LPS stimulation.

Drugs that can improve the autophagy of cardiomyocytes may ameliorate cardiac injury in sepsis (35,37). A previous study reported that valproic acid can accelerate autophagy in rats through the PTEN/AKT/mTOR pathway and relieve

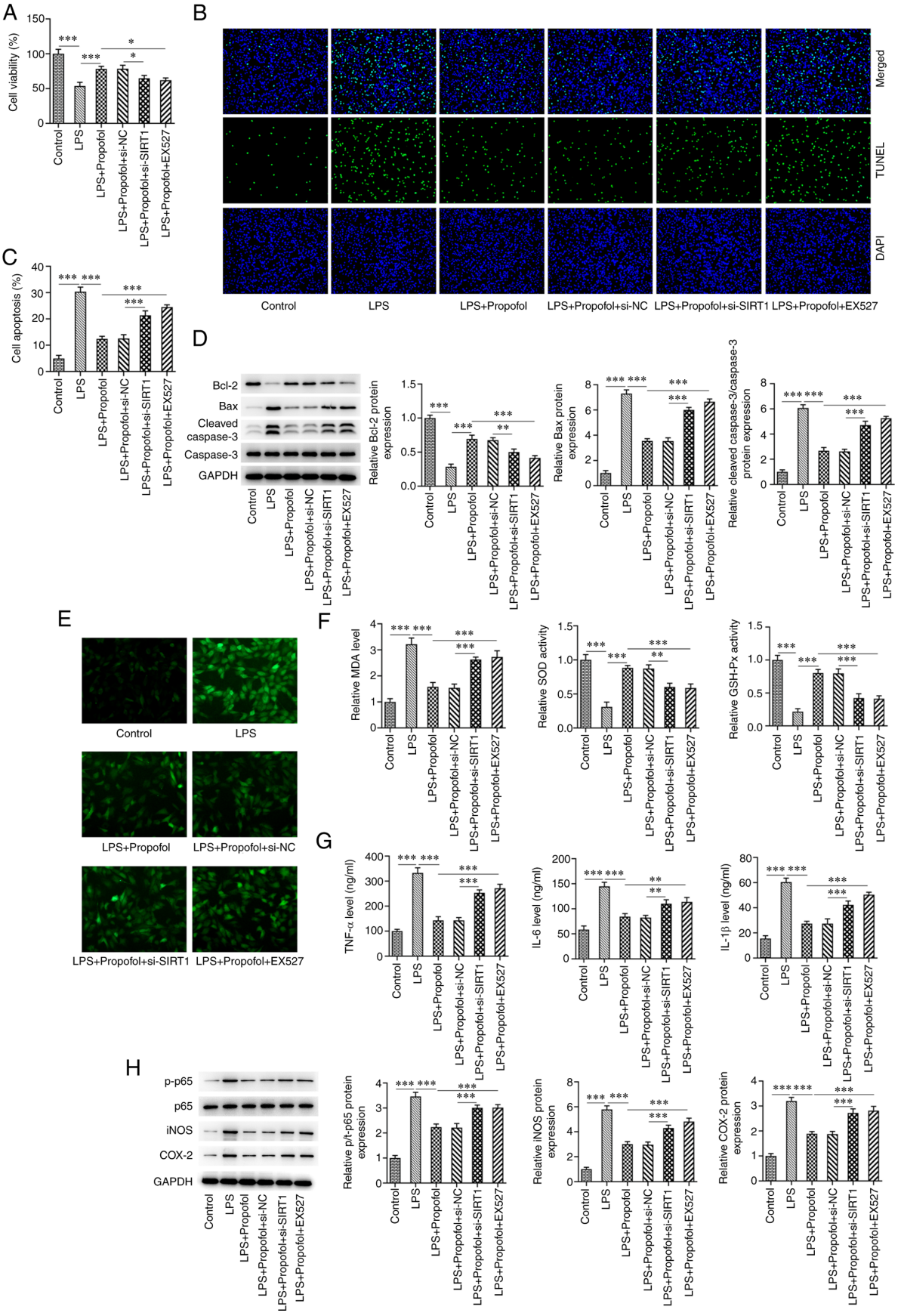

Figure 5. Inhibition of SIRT1 reduces the protective effect of propofol on LPS-induced cardiomyocytes. (A) Cell viability was measured using the Cell Counting Kit 8 assay. (B) Cell apoptosis was measured using the TUNEL assay. Magnification, x200. (C) Percentage of apoptotic cells. (D) Western blot analysis of the expression levels of Bcl-2, Bax, cleaved caspase-3 and caspase-3. (E) 2,7-dichlorohydrofluorescein diacetate staining assay for the detection of reactive oxygen species generation. Magnification, x200. (F) Levels of MDA content, SOD and GSH-Px activities. (G) ELISA of the levels of TNF-α, IL-6 and IL-1β. (H) Western blot analysis of the expression levels of p65, p-p65, iNOS and COX-2. *P<0.05, **P<0.01, ***P<0.001. LPS, lipopolysaccharide; GSH-Px, glutathione peroxidase; MDA, malondialdehyde; SOD superoxide dismutase; p-, phosphorylated; SIRT1, sirtuin 1; NC, negative control; si, small interfering.

cardiac dysfunction caused by sepsis (38). Pan *et al* (39) demonstrated that melatonin can regulate mitochondrial uncoupling protein, improve LPS-induced cardiac autophagy levels, protect the structure and function of mitochondria, and alleviate LPS-induced cardiac injury. Unuma *et al* (40) revealed that cobalt protoporphyrin can activate transcription factor EB and lysosomal-associated membrane protein in cardiomyocytes to promote autophagosome formation, protect cardiomyocytes and alleviate LPS-induced myocardial injury. It has been demonstrated that propofol can inhibit oxygen glucose deprivation and reperfusion-induced neuronal injury by inhibiting autophagy (41). The present study also hypothesized that propofol may regulate autophagy and serve a role in LPS-induced myocardial cell injury. Conversely, the experimental data demonstrated that after propofol treatment in LPS-induced cardiomyocytes, the expression levels of autophagy markers were increased, suggesting that propofol increased autophagy, which was consistent with a previous study, which suggested that propofol may serve a protective role in myocardial ischemia-reperfusion injury by inducing autophagy of cardiomyocytes through the stress-activated protein kinases/JNK pathway (42). Additionally, the present study demonstrated that, after propofol treatment in LPS-induced cardiomyocytes, the cell viability was increased, whereas the expression of oxidative stress markers and inflammatory factors were significantly decreased. Apoptosis is a process by which cells organize self-destruction. The mitochondrial apoptosis pathway is regulated by Bcl-2 family member proteins, including pro-apoptotic Bax, and anti-apoptotic Bcl-2 and Bcl-xL. Bax is able to enhance mitochondrial outer membrane permeability, thus leading to excessive release of cytochrome *c* and caspase-3 activation. Subsequently, caspase-3 activation participates in various apoptotic pathways, finally resulting in apoptosis (43). The present study detected the expression levels of Bcl-2, Bax and caspase-3 through western blotting and measured apoptosis through TUNEL assay, and demonstrated that propofol inhibited LPS-induced apoptosis of cardiomyocytes. These results suggested that propofol may improve myocardial cell injury by regulating autophagy. Subsequently, to further explore the mechanism of action, the effect of the autophagy inhibitor 3-MA was investigated and the results showed that 3-MA could significantly reverse the protective effect of propofol on myocardial cell injury.

SIRT1 is a key regulator of autophagy. A recent study reported that propofol can relieve the oxidative stress response of cerebral ischemia-reperfusion injury through the SIRT1 signaling pathway (44). In addition, SIRT1 inhibitors can decrease the protective effect of propofol on renal ischemia-reperfusion-mediated acute lung injury (45). Moreover, daming capsule, a hypolipidemic drug, promotes mitochondrial autophagy through the SIRT1/AMPK signaling pathway, thereby inhibiting myocardial cell injury and protecting against myocardial infarction (46). Quercetin has been shown to improve cardiomyocyte susceptibility to hypoxia by regulating SIRT1/TMBIM6-related mitochondrial autophagy and endoplasmic reticulum stress (47). The present study thus aimed to investigate whether propofol regulated myocardial cell injury by regulating SIRT1-mediated autophagy. In the present study, SIRT1 was silenced though siRNA transfection and inhibited using the SIRT1 inhibitor EX527. It was revealed that both silencing and inhibition of SIRT1 decreased propofol-induced autophagy and protected LPS-induced cardiomyocytes from injury. While normal autophagy protects cells, an excessive activation leads to cell damage; therefore, further investigation on the appropriate propofol dosage is required.

In conclusion, the present study indicated that propofol may reduce LPS-induced cardiomyocyte injury by activating SIRT1-mediated autophagy, implying that propofol may serve as a potential therapeutic agent for myocardial injury. However, the lack of detection of autophagosome formation is a limitation of the present study; therefore, further exploration is required to confirm the association between propofol and SIRT1-mediated autophagy in LPS-exposed cardiomyocytes.

Acknowledgements

Not applicable.

Funding

No funding was received.

Availability of data and materials

The datasets used and/or analyzed during the current study are available from the corresponding author on reasonable request.

Authors' contributions

JD and YZ designed the study and performed the experiments. YZ revised the manuscript for important intellectual content. JD collected and analyzed the data. JD and YZ confirm the authenticity of all the raw data. All authors read and approved the final manuscript.

Ethics approval and consent to participate

Not applicable.

Patient consent for publication

Not applicable.

Competing interests

The authors declare that they have no competing interests.

References

1. Merx MW and Weber C: Sepsis and the heart. Circulation 116: 793-802, 2007.
2. Romero-Bermejo FJ, Ruiz-Bailen M, Gil-Cebrian J and Huertos-Ranchal MJ: Sepsis-induced cardiomyopathy. Curr Cardiol Rev 7: 163-183, 2011.
3. Fan W, Zhu X, Wu L, Wu Z, Li D, Huang F and He H: Propofol: An anesthetic possessing neuroprotective effects. Eur Rev Med Pharmacol Sci 19: 1520-1529, 2015.
4. Li YM, Sun JG, Hu LH, Ma XC, Zhou G and Huang XZ: Propofol-mediated cardioprotection dependent of microRNA-451/HMGB1 against myocardial ischemia-reperfusion injury. J Cell Physiol 234: 23289-23301, 2019.

5. Lai HC, Yeh YC, Wang LC, Ting CT, Lee WL, Lee HW, Wang KY, Wu A, Su CS and Liu TJ: Propofol ameliorates doxorubicin-induced oxidative stress and cellular apoptosis in rat cardiomyocytes. Toxicol Appl Pharmacol 257: 437-448, 2011.
6. Lu Z, Liu Z and Fang B: Propofol protects cardiomyocytes from doxorubicin-induced toxic injury by activating the nuclear factor erythroid 2-related factor 2/glutathione peroxidase 4 signaling pathways. Bioengineered 13: 9145-9155, 2022.
7. Bao HG and Li S: Effects of propofol on the outcomes of rats with sepsis. J Surg Res 168: e111-e115, 2011.
8. Zhao H, Gu Y and Chen H: Propofol ameliorates endotoxininduced myocardial cell injury by inhibiting inflammation and apoptosis via the PPARgamma/HMGB1/NLRP3 axis. Mol Med Rep 23: 176, 2021.
9. Liu Z, Meng Y, Miao Y, Yu L and Yu Q: Propofol reduces renal ischemia/reperfusion-induced acute lung injury by stimulating sirtuin 1 and inhibiting pyroptosis. Aging (Albany NY) 13: 865-876, 2020.
10. Liu Y, Du X, Zhang S, Liu X and Xu G: Propofol alleviates hepatic ischemia/reperfusion injury via the activation of the Sirt1 pathway. Int J Clin Exp Pathol 10: 10959-10968, 2017.
11. Wang J, Qi J, Wu Q, Jiang H, Yin Y, Huan Y, Zhao Y and Zhu M: Propofol attenuates high glucose-induced P66shc expression in human umbilical vein endothelial cells through Sirt1. Acta Biochim Biophys Sin (Shanghai) 51: 197-203, 2019.
12. Wang L, Xu C, Johansen T, Berger SL and Dou Z: SIRT1-a new mammalian substrate of nuclear autophagy. Autophagy 17: 593-595, 2021.
13. Luo G, Jian Z, Zhu Y, Zhu Y, Chen B, Ma R, Tang F and Xiao Y: Sirt1 promotes autophagy and inhibits apoptosis to protect cardiomyocytes from hypoxic stress. Int J Mol Med 43: 2033-2043, 2019.
14. Zhang WX, He BM, Wu Y, Qiao JF and Peng ZY: Melatonin protects against sepsis-induced cardiac dysfunction by regulating apoptosis and autophagy via activation of SIRT1 in mice. Life Sci 217: 8-15, 2019.
15. Guo XN and Ma X: The effects of propofol on autophagy. DNA Cell Biol 39: 197-209, 2020.
16. Wang Y, Yu W, Shi C and Hu P: Crocetin attenuates sepsis-induced cardiac dysfunction via regulation of inflammatory response and mitochondrial function. Front Physiol 11: 514, 2020.
17. Tang J, Hu JJ, Lu CH, Liang JN, Xiao JF, Liu YT, Lin CS and Qin ZS: Propofol inhibits lipopolysaccharide-induced tumor necrosis factor-alpha expression and myocardial depression through decreasing the generation of superoxide anion in cardiomyocytes. Oxid Med Cell Longev 2014: 157376, 2014.
18. Yuan X, Chen G, Guo D, Xu L and Gu Y: Polydatin alleviates septic myocardial injury by promoting SIRT6-mediated autophagy. Inflammation 43: 785-795, 2020.
19. Xu C, Xiao Z, Wu H, Zhou G, He D, Chang Y, Li Y, Wang G and Xie M: BDMC protects AD in vitro via AMPK and SIRT1. Transl Neurosci 11: 319-327, 2020.
20. Livak KJ and Schmittgen TD: Analysis of relative gene expression data using real-time quantitative PCR and the 2(-Delta Delta C(T)) method. Methods 25: 402-408, 2001.
21. Lv X and Wang H: Pathophysiology of sepsis-induced myocardial dysfunction. Mil Med Res 3: 30, 2016.
22. Giordano NP, Cian MB and Dalebroux ZD: Outer membrane lipid secretion and the innate immune response to gram-negative bacteria. Infect Immun 88: e00920-19, 2020.
23. Abel FL: Myocardial function in sepsis and endotoxin shock. Am J Physiol 257: R1265-R1281, 1989.
24. Norouzi F, Abareshi A, Asgharzadeh F, Beheshti F, Hosseini M, Farzadnia M and Khazaei M: The effect of Nigella sativa on inflammation-induced myocardial fibrosis in male rats. Res Pharm Sci 12: 74-81, 2017.
25. Tung CL, Ju DT, Velmurugan BK, Ban B, Dung TD, Hsieh DJ, P Viswanadha V, Day CH, Lin YM and Huang CY: Carthamus tinctorius L. extract activates insulin-like growth factor-I receptor signaling to inhibit FAS-death receptor pathway and suppress lipopolysaccharides-induced H9c2 cardiomyoblast cell apoptosis. Environ Toxicol 34: 1320-1328, 2019.
26. Snezhkina AV, Kudryavtseva AV, Kardymon OL, Savvateeva MV, Melnikova NV, Krasnov GS and Dmitriev AA: ROS Generation and antioxidant defense systems in normal and malignant cells. Oxid Med Cell Longev 2019: 6175804, 2019.
27. Tsikas D: Assessment of lipid peroxidation by measuring malondialdehyde (MDA) and relatives in biological samples: Analytical and biological challenges. Anal Biochem 524: 13-30, 2017.
28. Diaz-Vivancos P, de Simone A, Kiddle G and Foyer CH: Glutathione-linking cell proliferation to oxidative stress. Free Radic Biol Med 89: 1154-1164, 2015.
29. Han B, Lv Z, Zhang X, Lv Y, Li S, Wu P, Yang Q, Li J, Qu B and Zhang Z: Deltamethrin induces liver fibrosis in quails via activation of the TGF-β1/Smad signaling pathway. Environ Pollut 259: 113870, 2020.
30. Yang X, Fang Y, Hou J, Wang X, Li J, Li S, Zheng X, Liu Y and Zhang Z: The heart as a target for deltamethrin toxicity: Inhibition of Nrf2/HO-1 pathway induces oxidative stress and results in inflammation and apoptosis. Chemosphere 300: 134479, 2022.
31. Jang DI, Lee AH, Shin HY, Song HR, Park JH, Kang TB, Lee SR and Yang SH: The role of tumor necrosis factor alpha (TNF-α) in autoimmune disease and current TNF-α inhibitors in therapeutics. Int J Mol Sci 22: 2719, 2021.
32. Li J, Yu Z, Han B, Li S, Lv Y, Wang X, Yang Q, Wu P, Liao Y, Qu B and Zhang Z: Activation of the GPX4/TLR4 signaling pathway participates in the alleviation of selenium yeast on deltamethrin-provoked cerebrum injury in quails. Mol Neurobiol 59: 2946-2961, 2022.
33. Galluzzi L and Green DR: Autophagy-independent functions of the autophagy machinery. Cell 177: 1682-1699, 2019.
34. Onorati AV, Dyczynski M, Ojha R and Amaravadi RK: Targeting autophagy in cancer. Cancer 124: 3307-3318, 2018.
35. Yin X, Xin H, Mao S, Wu G and Guo L: The role of autophagy in sepsis: Protection and injury to organs. Front Physiol 10: 1071, 2019.
36. Liu F, Nie C, Zhao N, Wang Y, Liu Y, Li Y, Zeng Z, Ding C, Shao Q, Qing C, *et al*: MiR-155 alleviates septic lung injury by inducing autophagy via inhibition of transforming growth factor-β-activated binding protein 2. Shock 48: 61-68, 2017.
37. Xie M, Morales CR, Lavandero S and Hill JA: Tuning flux: Autophagy as a target of heart disease therapy. Curr Opin Cardiol 26: 216-222, 2011.
38. Shi X, Liu Y, Zhang D and Xiao D: Valproic acid attenuates sepsis-induced myocardial dysfunction in rats by accelerating autophagy through the PTEN/AKT/mTOR pathway. Life Sci 232: 116613, 2019.
39. Pan P, Zhang H, Su L, Wang X and Liu D: Melatonin balance the autophagy and apoptosis by regulating UCP2 in the LPS-induced cardiomyopathy. Molecules 23: 675, 2018.
40. Unuma K, Aki T, Funakoshi T, Yoshida K and Uemura K: Cobalt protoporphyrin accelerates TFEB activation and lysosome reformation during LPS-induced septic insults in the rat heart. PLoS One 8: e56526, 2013.
41. Sun B, Ou H, Ren F, Huan Y, Zhong T, Gao M and Cai H: Propofol inhibited autophagy through Ca^{2+}/CaMKKβ/AMPK/mTOR pathway in OGD/R-induced neuron injury. Mol Med 24: 58, 2018.
42. Li H, Zhang X, Tan J, Sun L, Xu LH, Jiang YG, Lou JS, Shi XY and Mi WD: Propofol postconditioning protects H9c2 cells from hypoxia/reoxygenation injury by inducing autophagy via the SAPK/JNK pathway. Mol Med Rep 17: 4573-4580, 2018.
43. Li S, Wu P, Han B, Yang Q, Wang X, Li J, Deng N, Han B, Liao Y, Liu Y and Zhang Z: Deltamethrin induces apoptosis in cerebrum neurons of quail via promoting endoplasmic reticulum stress and mitochondrial dysfunction. Environ Toxicol 37: 2033-2043, 2022.
44. Liu XB, Xia H, Wang G, Zhang W, Hu Y and Zhang J: Propofol relieves oxidative stress response of cerebral ischemiareperfusion injury through SIRT1 signaling pathway. J Biol Regul Homeost Agents 34: 435-443, 2020.
45. Liu Z, Li C, Li Y, Yu L and Qu M: Propofol reduces renal ischemia reperfusion-mediated necroptosis by up-regulation of SIRT1 in rats. Inflammation 45: 2038-2051, 2022.
46. Sun X, Han Y, Dong C, Qu H, Yu Y, Ju J, Bai Y and Yang B: Daming capsule protects against myocardial infarction by promoting mitophagy via the SIRT1/AMPK signaling pathway. Biomed Pharmacother 151: 113162, 2022.
47. Chang X, Zhang T, Meng Q, ShiyuanWang, Yan P, Wang X, Luo D, Zhou X and Ji R: Quercetin improves cardiomyocyte vulnerability to hypoxia by regulating SIRT1/TMBIM6-related mitophagy and endoplasmic reticulum stress. Oxid Med Cell Longev 2021: 5529913, 2021.

This work is licensed under a Creative Commons Attribution-NonCommercial-NoDerivatives 4.0 International (CC BY-NC-ND 4.0) License.